Human Pathology 145 (2024) 48–55

Contents lists available at ScienceDirect

Human Pathology

journal homepage: www.elsevier.com/locate/humpath

Comprehensive phenotypic and genomic characterization of venous malformations

Katsutoshi Hirose, DDS, PhD [a], Yumiko Hori, MD, PhD [b,c,*], Michio Ozeki, MD, PhD [d], Daisuke Motooka, PhD [e], Kenji Hata, DDS PhD [f], Shinichiro Tahara, MD, PhD [b], Takahiro Matsui, MD, PhD [b], Masaharu Kohara [b], Kazuaki Maruyama, MD, PhD [g], Kyoko Imanaka-Yoshida, MD, PhD [g], Satoru Toyosawa, DDS, PhD [a], Eiichi Morii, MD, PhD [b]

[a] Department of Oral and Maxillofacial Pathology, Osaka University Graduate School of Dentistry, 1-8 Yamadaoka, Suita, Osaka, 565-0871, Japan
[b] Department of Pathology, Osaka University Graduate School of Medicine, 2-2 Yamadaoka, Suita, Osaka, 565-0871, Japan
[c] Department of Central Laboratory and Surgical Pathology, NHO Osaka National Hospital, 2-1-14 Hoenzaka, Chuo-ku, Osaka, 540-0006, Japan
[d] Department of Pediatrics, Graduate School of Medicine, Gifu University, 1-1 Yanagido, Gifu, Gifu, 501-1194, Japan
[e] Genome Information Research Center, Research Institute for Microbial Diseases, Osaka University, 3-1 Yamadaoka, Suita, Osaka, 565-0871, Japan
[f] Department of Molecular and Cellular Biochemistry, Osaka University Graduate School of Dentistry, 1-8 Yamadaoka, Suita, Osaka, 565-0871, Japan
[g] Department of Pathology and Matrix Biology, Mie University Graduate School of Medicine, 2-174 Edobashi, Tsu. Mie, 514-8507, Japan

ARTICLE INFO

Keywords:
TEK
PIK3CA
mTOR
Venous malformation
Sirolimus
Spatial transcriptomics

ABSTRACT

Venous malformations (VMs) are the most common vascular malformations. *TEK* and *PIK3CA* are the causal genes of VMs, and may be involved in the PI3K/AKT pathway. However, the downstream mechanisms underlying the *TEK* or *PIK3CA* mutations in VMs are not completely understood. This study aimed to identify a possible association between genetic mutations and clinicopathological features. A retrospective clinical, pathological, and genetic study of 114 patients with VMs was performed. *TEK*, *PIK3CA*, and combined *TEK/PIK3CA* mutations were identified in 49 (43%), 13 (11.4%), and 2 (1.75%) patients, respectively. *TEK*-mutant VMs more commonly occurred in younger patients than *TEK* and *PIK3CA* mutation-negative VMs (other-mutant VMs), and showed more frequent skin involvement and no lymphocytic aggregates. No significant differences were observed in sex, location of occurrence, malformed vessel size, vessel density, or thickness of the vascular smooth muscle among the VM genotypes. Immunohistochemical analysis revealed that the expression levels of phosphorylated AKT (p-AKT) were higher in the *TEK*-mutant VMs than those in *PIK3CA*-mutant and other-mutant VMs. The expression levels of p-mTOR and its downstream effectors were higher in all the VM genotypes than those in normal vessels. Spatial transcriptomics revealed that the genes involved in "blood vessel development", "positive regulation of cell migration", and "extracellular matrix organization" were up-regulated in a *TEK*-mutant VM. Significant genotype-phenotype correlations in clinical and pathological features were observed among the VM genotypes, indicating gene-specific effects. Detailed analysis of gene-specific effects in VMs may offer insights into the underlying molecular pathways and implications for targeted therapies.

1. Introduction

Vascular malformations are complex congenital vascular disorders which are classified according to their histological appearance [1–3]. Venous malformations (VMs), the most common type of vascular malformations (70 %), have an incidence of approximately 1–5 per 10, 000 births [2,3]. Histologically, VMs are characterized by ectatic venous-like vessels with a thin endothelial cells (ECs) lining, surrounded by sparse, erratically distributed vascular smooth muscle (VSM) and a disorganized extracellular matrix (ECM) [2,3]. Genetically, *TEK* and *phosphatidylinositol-4,5-bisphosphate 3-kinase catalytic subunit alpha*

* Corresponding author. Department of Central Laboratory and Surgical Pathology, NHO Osaka National Hospital, 2-1-14 Hoenzaka, Chuo-ku, Osaka, 540-0006, Japan.

E-mail addresses: hirose.katsutoshi.dent@osaka-u.ac.jp (K. Hirose), yumiko-hori@molpath.med.osaka-u.ac.jp (Y. Hori), ozeki.michio.j5@f.gifu-u.ac.jp (M. Ozeki), daisukem@gen-info.osaka-u.ac.jp (D. Motooka), hata.kenji.dent@osaka-u.ac.jp (K. Hata), s-tahara@molpath.med.osaka-u.ac.jp (S. Tahara), matsuit@molpath.med.osaka-u.ac.jp (T. Matsui), kohara@molpath.med.osaka-u.ac.jp (M. Kohara), k.maruyama0608@gmail.com (K. Maruyama), imanaka@med.mie-u.ac.jp (K. Imanaka-Yoshida), toyosawa@dent.osaka-u.ac.jp (S. Toyosawa), morii@molpath.med.osaka-u.ac.jp (E. Morii).

https://doi.org/10.1016/j.humpath.2024.02.004
Received 18 December 2023; Received in revised form 2 February 2024; Accepted 6 February 2024
Available online 15 February 2024

List of abbreviations

4EBP1	Eukaryotic translation initiation factor 4E-binding protein 1
AKT1	AKT serine/threonine kinase 1
EC	Endothelial cell
ECM	Extracellular matrix
EVG	Elastica van Gieson
FFPE	Formalin-fixed paraffin-embedded
LM	Lymphatic malformation
MAPK	Mitogen-activated protein kinase
mTOR	Mammalian target of rapamycin
NF-κB	Nuclear factor kappa light chain enhancer of activated B
PI3K	Phosphoinositide 3-kinase
PIK3CA	Phosphatidylinositol-4,5-bisphosphate 3-kinase catalytic subunit alpha
S6K1	Ribosomal protein S6 kinase 1
SMA	Smooth muscle actin
VEGF	Vascular endothelial growth factor
VM	Venous malformation
VSM	Vascular smooth muscle

(*PIK3CA*) mutations are present in approximately 50% and 20% of all VMs, respectively [4–8]. The remaining *TEK/PIK3CA* mutation-negative VMs might be caused by infrequent mutations in other genes [7,9]. *TEK* gene encodes for endothelial cell tyrosine kinase receptor TIE2 which participates in the regulation of angiogenesis, vessel maturation, and vascular integrity [10–12]. Gain-of-function mutations in *TEK* are unique to VM [1,11,12]. *PIK3CA* codes the p110a catalytic subunit of the phosphoinositide 3-kinase (PI3K), and gain-of function mutations in *PIK3CA* are closely related to the development of cancers and various vascular malformations [6–9]. Based on genetic data from previous studies, both genes have been accepted as causal genes for VMs [3,9,13–15].

The *TEK* or *PIK3CA* gene mutation occurs within ECs of VMs, and VM studies have focused on ECs *in vitro* using human umbilical vein endothelial cells or patient-derived ECs [13,15–18]. The *TEK* or *PIK3CA* mutations have been suggested to be involved in the pathogenesis of VMs via the PI3K/AKT pathway [6,13–15]. When transduced in cultured ECs, both *TEK* and *PIK3CA* mutations activate AKT, but only *TEK* mutations activate other pathway components such as STAT1 and ERK1/2 [6,13–15]. *TEK*-mutant-transduced ECs increase in number by extending their lifespan, rather than proliferating, *in vitro* and in mouse transplantation models [13–16]. On the other hand, *PIK3CA*-mutant--transduced ECs exhibited increased EC proliferation, with no decrease in the rate of apoptosis [7,8]. These findings suggested that some gene-specific effects may be present in VMs; thus, the clinicopathological phenotypes are thought to be different among the causal genes of VMs. A previous study revealed that *TEK/PIK3CA* mutation-negative VMs showed lower levels of D-dimer compared to *TEK*-mutant or *PIK3CA*-mutant VMs [6]. Moreover, *PIK3CA*-mutant VMs clinically displayed more deeper lesions that are not extending into the skin, in contrast to the common *TEK*-mutant VMs [6]. However, the other phenotype-genotype correlations in VMs remain unknown.

Recently, genetic studies have identified that the mutations associated with a large proportion of vascular malformations are involved with the PI3K/AKT/mammalian target of rapamycin (mTOR) or mitogen-activated protein kinase (MAPK)/ERK pathway [19,20]. Currently, many studies aim to understand the molecular and cellular consequences of these mutations and the prospects for targeted therapies in vascular malformations [19–23]. The mTOR inhibitor, sirolimus (also known as rapamycin), is an efficacious and safe therapeutic agent for the majority of patients with complicated various vascular anomalies including vascular tumors and malformations [21–23]. mTOR is one of the AKT downstream targets; PI3K/AKT/mTOR signaling pathway plays an important role in the development of various vascular malformations such as lymphatic malformations (LMs), fibro-adipose vascular anomaly, and PIK3CA-related overgrowth spectrum [24–27]. Sirolimus displayed clinical improvement in LMs [21–23], and has been recently approved in Japan for the treatment of LMs and related lymphatic disorders. The current treatment approaches of VMs are ablation of the abnormal vessels by sclerotherapy or removal by surgical excision; sirolimus is being tested as a novel therapeutic agent in several clinical trials for VMs [2,3,21,23]. However, the mTOR activation status in VMs was not previously studied, and the exact mechanism of action of sirolimus is not completely understood.

To explore the characteristics of VMs in relation to genetic mutations, this study investigated the correlations between the genetic mutational status, clinicopathological features, and expression of mTOR pathway components in a large series of VMs. Furthermore, we examined the mRNA gene expression patterns in the ECs of *TEK*- and *PIK3CA*-mutant VMs using spatial transcriptomics.

2. Patients and methods

2.1. Patients selection

Formalin-fixed paraffin-embedded (FFPE) tissues obtained through biopsy or resection from 114 patients with VMs were retrieved from the pathology files of Osaka University Hospital. All vascular malformations were classified according to the classification systems of the International Society for the Study of Vascular Anomalies [1]. The final diagnosis of VM was confirmed by two pathologists (K.H. and Y.H.). This study was approved by the Ethical Review Board of the Graduate School of Medicine, Osaka University (IRB No. 17214). The requirement for informed consent was waived by the Ethical Review Board.

2.2. Mutation analysis

Next-generation sequencing was performed using a custom panel, as previously described [26]. Genomic DNA was extracted from FFPE tissues using the QIAamp DNA FFPE Tissue Kit (Qiagen, Valencia, CA, USA). The gene panel was designed using SureDesign (https://earray.chem.agilent.com/suredesign. Accessed Dec 10, 2023) to cover all the exons of *TEK* and *PIK3CA* genes. Sequence libraries were prepared using the custom SureSelect Low-Input Target Enrichment System (Agilent Technologies Inc. Santa Clara, CA, USA), and sequenced using Illumina MiSeq (Illumina, San Diego, CA, USA). SureCall ver4.0 (https://www.agilent.com/en/download-software-surecall. Accessed Dec 10, 2023) was used for the variant calling. Intron DNA, non-coding DNA, and variant allele frequency <1% were excluded. Variants obtained by panel sequencing were confirmed by Sanger sequencing, as previously described [26].

2.3. Histological and immunohistochemical analysis

Resected tissue samples were fixed with 10% formalin, routinely embedded in paraffin, cut into 4-μm thick serial sections, and used for Hematoxylin-Eosin, Elastica van Gieson (EVG), and immunohistochemical staining. Immunohistochemical staining was performed using Roche Ventana BenchMark GX autostainer (Ventana Medical Systems, Tucson, AZ, USA). Primary antibodies against, αSMA (clone 1A4, 1:500; Dako, Denmark), phosphorylated AKT (p-AKT) (#4060, 1:100; Cell Signaling Technology, Danvers, MA, USA), p-mTOR (clone 49F9, 1:100; Cell Signaling Technology), p-4EBP1 (clone 236B4, 1:500; Cell Signaling Technology), p-S6K1 (#9204, 1:100; Cell Signaling Technology), and SP1 (#84386, 1:1600; Cell Signaling Technology) were used. The expression levels of those proteins were assessed by two pathologists (K.H. and Y.H.) using a visual grading system based on the staining

intensity observed under a light microscope. Undetectable, weak, moderate, and strong staining were defined as negative (score 0), low (score 1), intermediate (score 2), and high (score 3), respectively. H-scores were calculated using the following formula: H-score = (0 (% cells with score 0) + 1 (% cells with score 1) + 2 (% cells with score 2) + 3 (% cells with score 3)). The blood vessel diameter was classified into ≥1 cm (large vessels), <1 cm (small vessels), or a combination of those sizes; the VSM thickness was classified into thick, thin, few, or a mixture of those thicknesses; and the elastic fibers within the malformed vessel walls were classified into positive (+), focal (±; partially positive), and negative (-; almost nothing).

2.4. Spatial transcriptomics

Resected tissue samples were fixed with 10% formalin, routinely embedded in paraffin, and cut into 5-μm thick sections. Visium libraries were prepared according to the Visium Spatial Gene Expression User Guide and then sequenced on DNBSEQ-G400RS (MGI). The raw FASTQ files and histological images were processed using Space Ranger software (v2.1.1). The raw Visium files for each sample were read using Loupe Browser software (v6.0.0) to visualize the spatial expression using histological images. We obtained 118,004,147 and 128,774,256 sequence read counts and identified 1280 and 2743 median genes per spot in *TEK*-mutant and *PIK3CA*-mutant VMs, respectively. We examined up-regulated genes compared to TEK-vessels and Normal-vessels, or compared to PIK3CA-vessels and Normal-vessels within each VM. Gene ontology enrichment analysis was performed using Metascape (https://metascape.org/. Accessed Dec 10, 2023) to elucidate the biological functions of the up-regulated genes identified using spatial transcriptomics.

2.5. Statistical analyses

The data are expressed as means ± standard deviations. Statistical analyses and graph creation were performed using Microsoft Excel and GraphPad Prism (version 10; La Jolla, CA, USA). Statistical significance was set at a p-value <0.05. The data were tested using Steel–Dwass's multiple comparison test, Fisher's exact test, Kruskal–Wallis test, and

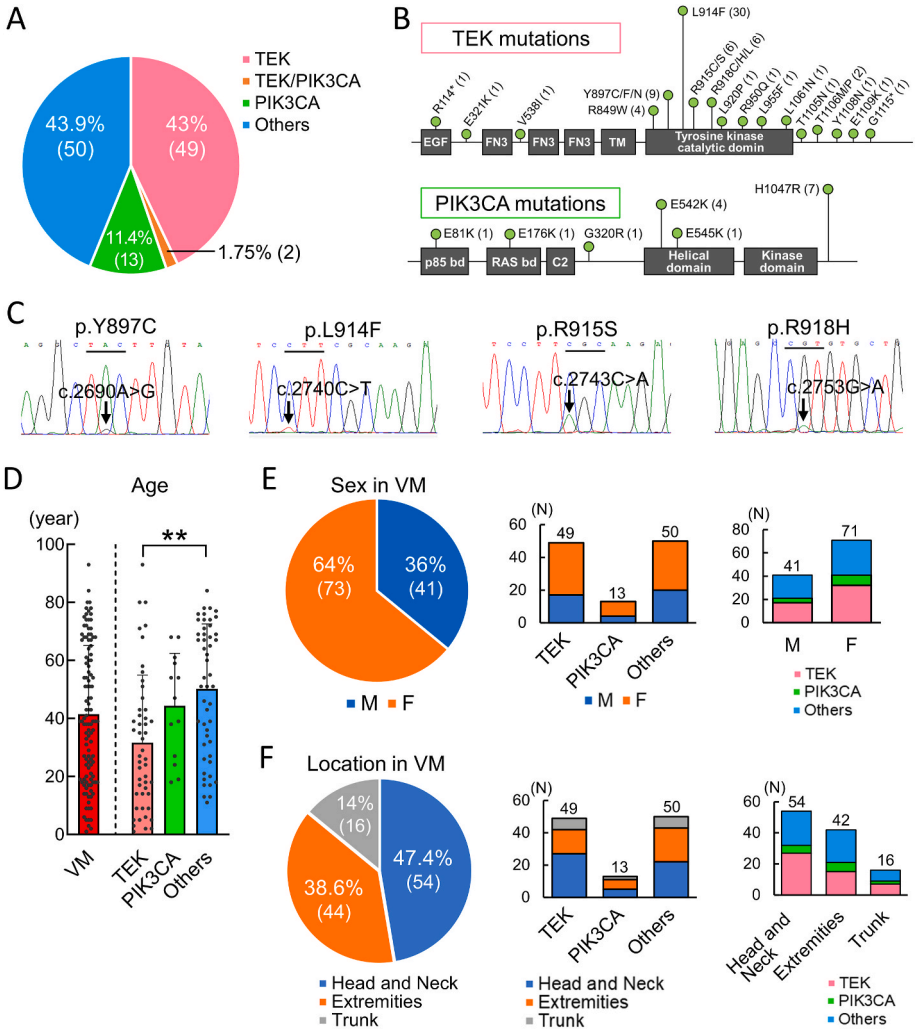

Fig. 1. Molecular genetic analysis and association with clinical features in venous malformations **A.** Pie chart showing the contribution of mutant genes in venous malformations (VMs). **B.** The occurrence and distribution of various *TEK* mutation sites (upper) and *PIK3CA* mutation sites (lower). **C.** Direct gene sequencing showing chromatograms for *TEK* mutations; p.Y897C (c.2690A > G), p.L914F (c.2740C > T), p.R915S (c.2743C > A), and p.R918H (c.2753G > A). **D.** Age distribution in relation to mutation types (red; all VMs, pink; *TEK*-mutant VMs, green; *PIK3CA*-mutant VMs, blue; other-mutant VMs). The points indicate the ages of individual patients. **E.** Pie chart showing the sex distribution of VMs (left), sex distribution in relation to mutation types (middle), and mutation type distribution in relation to sex (right). **F.** Pie chart showing the location distribution of VMs (left), location distribution in relation to mutation types (middle), and mutation type distribution in relation to location (right). P values were determined by Steel–Dwass's multiple comparison test (for age) or Kruskal–Wallis test (for other parameters). p** <0.01. (For interpretation of the references to colour in this figure legend, the reader is referred to the Web version of this article.)

Spearman's rank correlation test.

3. Results

3.1. TEK and PIK3CA mutational analyses

Next-generation sequencing was performed for 114 patients with VMs, and the mutations were detected in 64 patients (56.14%) (Fig. 1A). *TEK, PIK3CA*, and combined *TEK* and *PIK3CA* mutations were detected in 49 (43%), 13 (13%), and 2 (1.75%) patients, respectively. Neither *TEK* nor *PIK3CA* mutations were detected in the other 50 patients (43.9%); thus, they were classified as having other-mutant VMs. Sixty-eight *TEK* mutations were detected in 51 patients: p.L914F (n = 30) was the most frequent mutation, followed by p.Y897C/F/N (n = 9), p.R915C/S (n = 6), and p.R918C/H/L (n = 6) (Fig. 1B and C). *TEK* mutations were exclusively detected in exon 17 and were located within the tyrosine kinase and kinase insert domains of the receptor (Fig. 1B). Most TEK^{L914F}-mutant VMs had a single *TEK* p.L914F mutation, whereas $TEK^{Non\text{-}L914F}$-mutant VMs had ≥2 *TEK* mutations in one patient (Supplemental Fig. 1A). Most double *TEK* mutations in $TEK^{Non\text{-}L914F}$-mutant VMs were associated with p.Y897, p.R915, or p.R918 mutations. *PIK3CA* mutations were detected in 15 patients: p.H1047R (n = 7) was the most frequent mutation, followed by p.E542K (n = 4) (Fig. 1B). The identified *PIK3CA* mutations were termed hotspot mutations: p.E542 and p.E545 in the helical domain (exon 9) and p.H1047 in the kinase domain (exon 20).

3.2. Clinical features

We evaluated 114 patients with a mean age of 41.43 years (1–93 years) and a male-to-female ratio of 1:1.78 (36% males and 64% females) (Fig. 1D and E). VMs were located in the head and neck region (47.4%), followed by upper and lower extremities (38.6%), and trunk (14%) (Fig. 1F). The mean ages of patients with *TEK*-, *PIK3CA*-, and other-mutant VMs were 31.72 (1–93), 42.09 (18–68), and 49.91 (11–84) years, respectively (Fig. 1D). In younger patients, *TEK*-mutant VMs occurred more often than other-mutant VMs (Fig. 1D). All patients aged <10 years (11/11 patients) and almost half of the teenagers (8/15 patients) had *TEK* mutations. The male-to-female ratio and locations were not significantly different among the VMs (Fig. 1E and F). Age, male-to-female ratio, and location did not differ between TEK^{L914F}- and $TEK^{Non\text{-}L914F}$-mutant VMs (Supplemental Fig. 1A).

3.3. Histological features

No significant differences were observed in the vessel diameter,

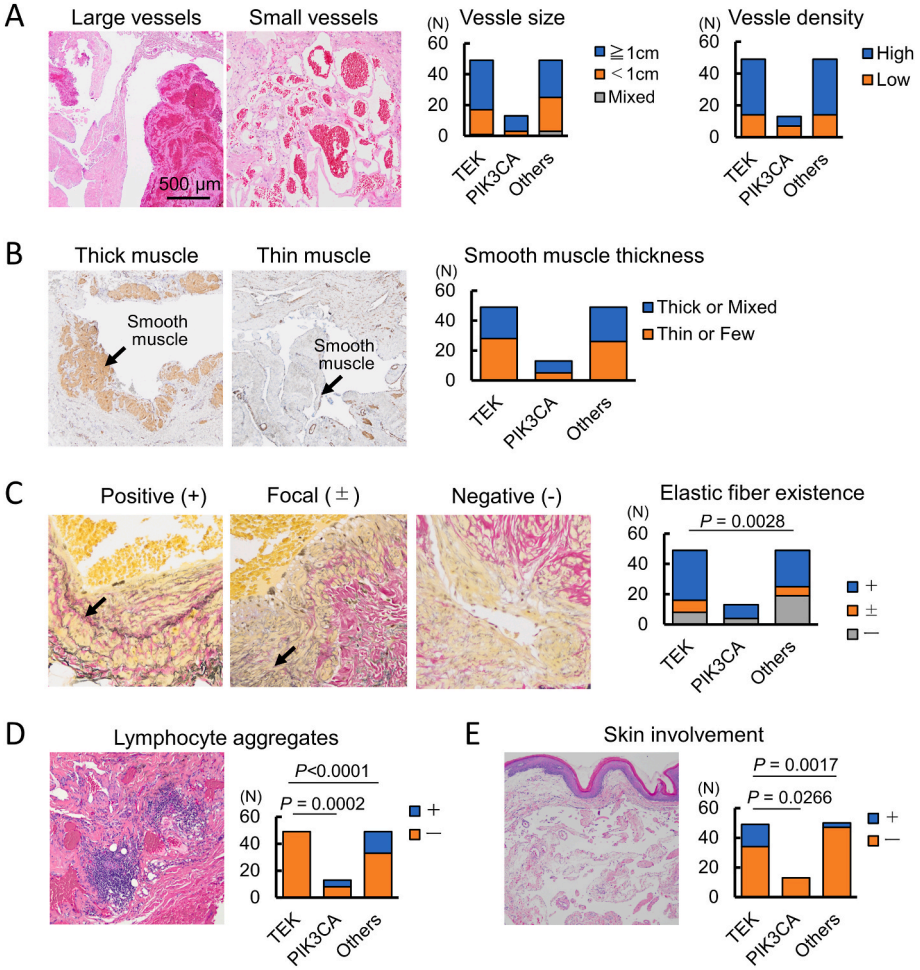

Fig. 2. Histological and immunohistochemical analyses of venous malformations **A.** Representative histological findings of large and small vessels and the distribution of vessel size and density in relation to mutation types. **B.** Representative αSMA staining showing thick and thin vascular smooth muscles and the distribution of smooth muscle thickness in relation to mutation types. The arrows indicate the αSMA-positive vascular smooth muscles. **C.** Representative Elastica van Gieson staining showing elastic fiber existence and the distribution of elastic fiber existence in relation to mutation types. The arrows indicate the elastic fibers. **D and E.** Representative histological findings of lymphocytic aggregates (excluding those caused by vascular rupture or phlebolith) and skin dermis involvement, and these distributions in relation to the mutation types. P-values were determined by the Kruskal–Wallis test or Fisher's exact test.

vessel density, and VSM thickness among the VM genotypes (Fig. 2A and B). *TEK*-mutant VMs had more elastic fibers (+and ±; 41/49 patients) than other-mutant VMs (+and ±; 30/50 patients) (Fig. 2C). Lymphocytic aggregates (excluding those caused by vascular rupture or phlebolith) appeared in 0% (0/49 patients), 38.46% (5/13 patients), 32.0% (16/50 patients) of *TEK*-, *PIK3CA*-, and other-mutant VMs, respectively (Fig. 2D). *TEK*-mutant VMs had more skin dermis involvement (30.61%, 15/49 patients) than *PIK3CA*- (0%, 0/13 patients) and other- (6%, 3/50 patients) mutant VMs (Fig. 2E). These histological parameters did not differ between the TEK^{L914F}- and $TEK^{Non\text{-}L914F}$-mutant VMs.

3.4. mTOR pathway components expression

We analyzed the expression of four proteins that play important roles in the PI3K/AKT/mTOR pathway. The expression levels of p-AKT were higher in the *TEK*-mutant than those in the *PIK3CA*- and other-mutant VMs (Fig. 3B). The expression levels of p-mTOR and phosphorylated downstream mTOR effectors, such as eukaryotic translation initiation factor 4E-binding protein 1 (4EBP1) and ribosomal protein S6 kinase 1 (S6K1), were not significantly different among the VM genotypes (Fig. 3B). In normal vessels, p-AKT, p-mTOR, and p-4EBP1 were undetectable, whereas p-S6K1 was sporadically expressed at low levels (Fig. 3C). The expression levels in normal vessels were lower than those in malformed vessels for each VM genotype (Fig. 3B and C).

3.5. Transcriptomic profiles

Spatial transcriptomics was performed for a TEK^{L914F}- and a $PIK3CA^{E545K}$-mutant VM (Fig. 4A). The two VMs showed similar findings regarding age, sex, location, large vessels, and thick VSM (Fig. 4A). The *CD31* (marker for ECs) mRNA was highly expressed in "TEK-vessels", "PIK3CA-vessels", and "Normal-vessels", with no significant difference among them (Fig. 4B). The *podoplanin* (marker for lymphatic vessels) mRNA was minimally expressed (Fig. 4B). We identified 191 and 27 genes that were highly expressed in TEK-vessels and PIK3CA-vessels, respectively (Fig. 4C–Supplemental Table 1). Gene ontology analysis was performed to investigate the functions of the 190 up-regulated genes which were identified only in TEK-vessels (Supplemental Table 2). The findings revealed that the genes were mainly involved in "blood vessel development", "positive regulation of cell migration", and "extracellular matrix organization" (Fig. 4C). The top three transcription factors regulating these genes were SP1 (gene count = 20; $Log_{10}(P) = -9.8$), RELA (gene count = 29; $Log_{10}(P) = -13$), and NF-κB (gene count = 20; $Log_{10}(P) = -13$). SP1 was highly expressed in the ECs and weakly expressed in some VSM cells of *TEK*-mutant VMs (Fig. 4E). SP1 expression in the ECs of *TEK*-mutant VMs was positively correlated with p-AKT expression (r = 0.5183; p = 0.00033) (Fig. 4F). On the contrary, SP1 expression in the ECs of *PIK3CA*-mutant VMs was not correlated with p-AKT expression (r = 0.2198; p = 0.4464) (Fig. 4F).

4. Discussion

The present study reported the largest VM series of comprehensive clinical, histological, immunohistochemical, and genetic analyses. *TEK* and *PIK3CA* are the most important genes whose mutations are related to VM development [3,9,13–15]. Du et al. (2021) reviewed 300 VM cases in eight studies [9]. The prevalence of *TEK* mutations, *PIK3CA* mutations, and combined *TEK* and *PIK3CA* mutations was 41.3% (62/150), 26.7% (40/150) and 1.3% (2/150), respectively [9]. In *TEK* mutation, p.L914F was most frequent mutation site, followed by p.Y897, p.R915, and p.R918 [9]. In *PIK3CA* mutation, p.H1047 was most frequent site, followed by p.E542 and p.E545 [9]. These *TEK* and *PIK3CA* mutational statuses in VMs which were reported by previous studies were compatible with the findings of our present study (Fig. 1A and B). We revealed that some clinicopathological findings were not common among *TEK*-mutant, *PIK3CA*-mutant and other-mutant VMs. In

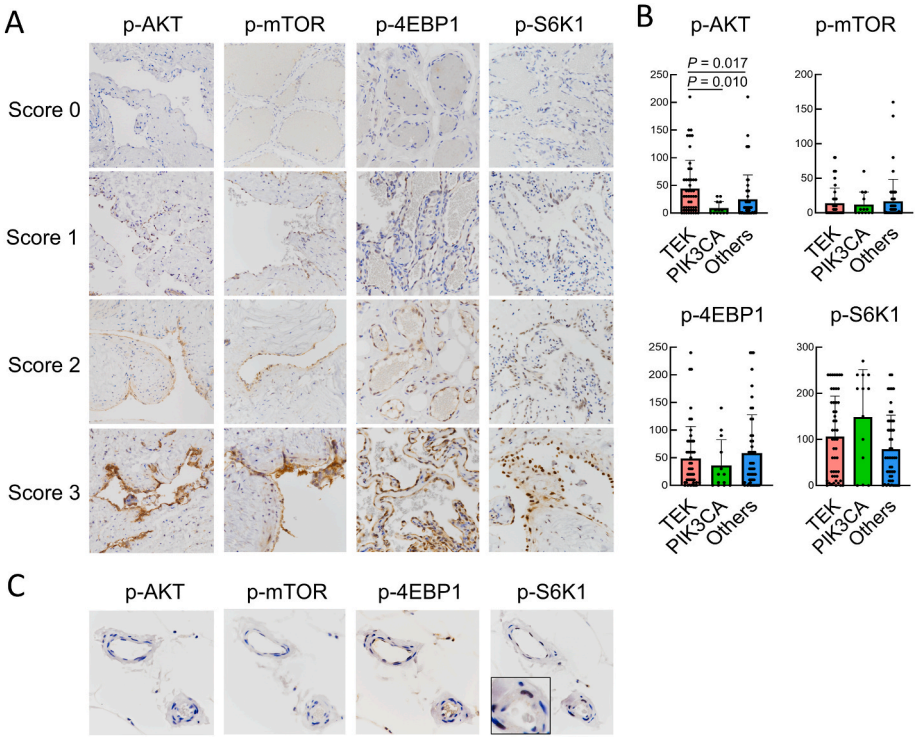

Fig. 3. Immunohistochemical analyses of the expression of mTOR pathway components in venous malformations **A.** Representative immunohistochemical staining patterns of phosphorylated AKT (p-AKT), p-mTOR, p-4EBP1, and p-S6K1. **B.** The distribution of the expression levels of these mTOR pathway components in relation to mutation types. **C.** Representative immunohistochemical staining patterns of mTOR pathway components in normal vessels. P-values were determined by Steel–Dwass's multiple comparison test. mTOR; mammalian target of rapamycin, 4EBP1; eukaryotic translation initiation factor 4E-binding protein 1, S6K1; ribosomal protein S6 kinase 1.

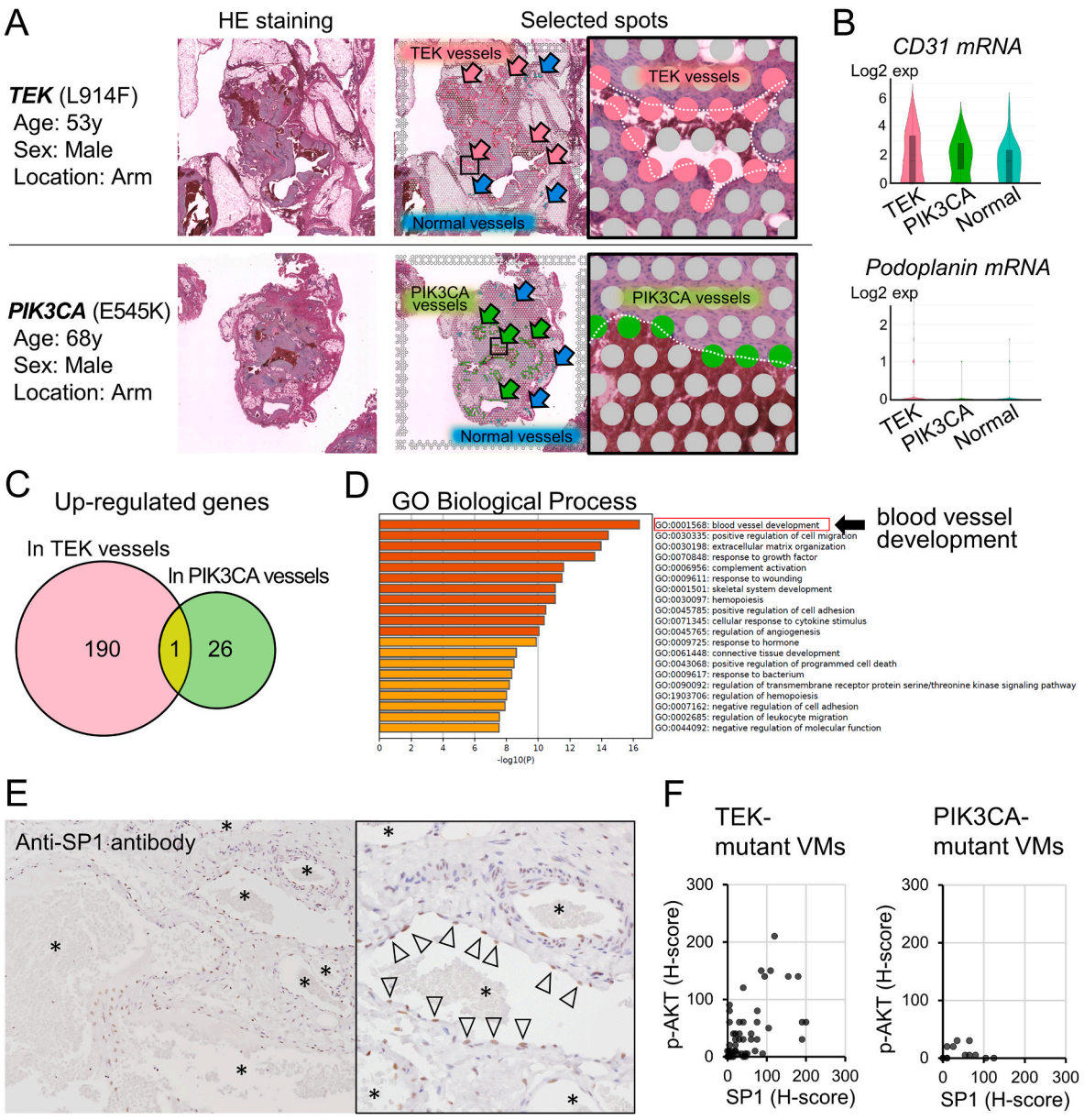

Fig. 4. Spatial transcriptomics in venous malformations **A**. Hematoxylin-Eosin staining (left column) and Selected spots (right column) in a *TEK*-mutant venous malformation (VM) (upper line) and a *PIK3CA*-mutant VM (lower line). "TEK-vessels" (pink arrows and circles) and "PIK3CA-vessels" (green arrows and circles) indicate selected spots of endothelial cells (ECs) of malformed vessels in *TEK*-mutant VM and *PIK3CA*-mutant VM, respectively. "Normal-vessels" (blue arrows and circles) indicate selected spots of typical normal vessels. Black line boxes indicate higher magnification. **B**. The expression levels of *CD31* (maker for ECs) and *podoplanin* (marker for lymphatic vessels) in three types of vessels. **C**. The up-regulated genes in TEK-vessels or PIK3CA-vessels compared to those in Normal-vessels. **D**. Gene Ontology (GO) enrichment analysis of the up-regulated genes in TEK-vessels. **E**. Representative immunohistochemical staining of SP1 in *TEK*-mutant VM (asterisks, lumen of malformed vessels; black line-box, higher magnification; arrows, ECs of malformed vessel). **F**. Scatterplot of AKT/SP1 scores from *TEK*-mutant VMs (left) and *PIK3CA*-mutant VMs (right). The points indicate immunoreactivity values in individual VM cases. P-values were determined by Spearman's rank correlation coefficient. (For interpretation of the references to colour in this figure legend, the reader is referred to the Web version of this article.)

particular, *TEK*-mutant VMs had distinct clinicopathological features. *TEK*-mutant VMs occurred more often in younger patients, especially those younger than 10 years (Fig. 1D). Histologically, *TEK*-mutant VMs showed more skin involvement, unlike *PIK3CA*-mutant and other-mutant VMs which rarely showed skin involvement (Fig. 2E). Limaye et al. suggested that differences in the location and timing of mutation acquisition result in these phenotypic differences [6]. In addition, the *TEK*-mutant VMs never showed lymphocytic aggregates, whereas *PIK3CA*-mutant and other-mutant VMs occasionally exhibited lymphocytic aggregates (Fig. 2D). The *PIK3CA* mutation associated vascular malformations such as LMs and fibro-adipose vascular anomaly (complex lymphatic-venous malformation) often showed lymphocytic aggregates, and *PIK3CA* mutations in ECs may influence the lymphocytic infiltration [1,24,26]. This present study showed significant genotype-phenotype correlations in the clinical and pathological features, and these features could suggest and support the presence of specific mutations in VMs.

VMs are complexes of ectatic venous-like vessels surrounded by VSM and disorganized ECM. To our knowledge, this present study is the first to report transcriptomics of ECs in VM lesions *in vivo*. Compared to PIK3CA-vessels and Normal-vessels, TEK-vessels showed upregulation of the genes involved in blood vessel development, positive regulation of cell migration, and ECM organization (Fig. 4C). In a previous *in vitro* study, the *TEK* p.L914F mutation in cultured ECs dysregulated the genes

involved in vascular development, cell migration and ECM processing [16]. *TEK*-mutant-derived ECs or patient-derived ECs harboring *TEK* mutations which were transplanted into xenograft nude mice formed VM-like lesion, which are ectatic blood-filled vessels with scarce smooth muscle cell coverage [14,15]. These results supported that the mutations in ECs not only affect the EC intrinsic functions, but also EC–VSM interactions and perivascular ECM disorganization [3,13–15]. Our transcriptomics findings revealed that many candidate genes were involved in VM development (Fig. 4C and D). The SP1, RELA (Nuclear factor kappa light chain enhancer of activated B [NF-κB] p65 Subunit), and NF-κB were the top three transcriptional factors that regulate highly expressed genes in TEK-vessels. The involvement of these transcriptional factors in VM development is unreported. In angiogenesis, the SP1-dependent transcriptional regulation of vascular endothelial growth factor (VEGF) expression through AKT activation [28]. VEGF is an important mediator of angiogenesis in a variety of settings [28]. SP1 was highly expressed in the ECs of the malformed vessels, and SP1-AKT axis was observed in *TEK*-mutant VMs (Fig. 4E and F). AKT is a central player in several signaling pathways and regulates cell growth, proliferation, survival, and various aspects of intermediary metabolism [16,18,27–29]. AKT activation in VMs is linked to increased survival of ECs and VSM recruitment [29]. Further studies are needed to determine whether the SP1-AKT axis is involved in VM development. The analysis of the identified genes by *in vivo* and *in vitro* transcriptomics may lead to a more detailed understanding of the VM development mechanism.

The mTOR inhibitor sirolimus is an efficacious novel therapeutic agent for unresectable vascular anomalies [21–23]. The mTOR signaling pathway, an important intracellular pathway, plays a major role in cell growth, metabolism, and apoptosis. It is involved in various pathological mechanisms of angiogenesis, lymphangiogenesis, and development of several cancers [24–27]. To our knowledge, the present study is the first to report the expression of mTOR pathway components in VMs (Fig. 3). We demonstrated that mTOR pathway was highly activated in malformed vessels of VMs having any of the three genotypes compared to that in normal vessels (Fig. 3B and C). These results may provide therapeutic evidence for the use of sirolimus in VM treatment. A detailed protein expression analysis of the mTOR pathway components may shed light on their roles in VMs, and predict their clinical prognosis. Further studies are needed to determine whether it is possible to predict which patients will benefit from sirolimus treatment and whether the expression levels of the mTOR pathway components can serve as biomarkers of treatment response.

Sirolimus is effective for various vascular anomalies; some studies reported that sirolimus treatment seemed more effective for LMs than that for VMs [21,23]. In LMs harboring *PIK3CA* mutation, sirolimus decreased the LM volume, oozing, and bleeding, which in turn increased the quality of life [21,23]. In VMs harboring *TEK* mutations, sirolimus improved the symptoms such as pain and bleeding, but did not reduce the VM volume [21,23]. In clinical use, long-term treatment with sirolimus may cause significant side-effects; it has potent immunosuppressant actions and cannot completely regress the VM lesions [3,13,14,23]. The reason why sirolimus is less effective against VMs harboring *TEK* mutations is unknown. One possibility is that the difference in the therapeutic effects may be attributed to downstream pathways other than mTOR from *TEK* mutations. Activating mutations in *TEK* or *PIK3CA* induce abnormal activation of the PI3K/AKT signaling pathway in cultured ECs, but only *TEK* mutations cause phosphorylation of STAT1 and ERK1/2 within MAPK/ERK pathway [7,8,13–15]. Sirolimus mildly inhibited p-AKT, and did not significantly affect both p-STAT1 and p-ERK1 levels in ECs harboring *TEK* mutations [11,12,14]. The combination of sirolimus and ponatinib regressed cultured ECs harboring *TEK* mutations or xenograft mice model better than sirolimus alone [17]. Ponatinib is a tyrosine kinase inhibitor that is considered as suppress TIE2 and MAPK/ERK signaling pathway in VMs [17]. The downstream pathway analysis of *TEK* or *PIK3CA* mutations in VMs may identify potential genetic mechanism and selected targeted medicines in the future. The spatial transcriptomic findings revealed by our study which showed that most of the up-regulated genes were not common between *TEK*-mutant and *PIK3CA*-mutant VMs (Fig. 4C) should lead to understanding the difference in the downstream pathways of *TEK* or *PIK3CA* mutations.

The present study has some limitations. First, the treatment history, such as sclerotherapy or administration of medications before the resection of the VM lesions, was not considered. This is attributed to the complex treatment strategies which differ depending on the patient age and disease location. Second, the present study is a single-center case analysis. However, clinical aspects such as the proportion of gender and location of VMs, as well as aspects of genetic mutations in VMs, were generally consistent within this study and previous reports [2,3,9]. Third, spatial transcriptomics was performed for only one *TEK*-mutant and *PIK3CA*-mutant VM each (Fig. 4A). Further accumulation of transcriptomic data in VMs is required to determine the association between the mutations and mRNA gene expression patterns. Fourth, *TEK/PIK3CA* mutation-negative VMs, which constituted half of all VMs, are likely caused by infrequent mutations in several genes associated with PI3K/AKT and MAPK/ERK signaling pathways, as suggested by Castel et al. [7,19,20]. Further genetic studies on these patients would provide critical support for the current genetic theory of VMs pathogenesis. Exploring the mechanism of VMs remains a major challenge and must be continued in the future.

5. Conclusions

Significant genotype-phenotype correlations in the clinical and pathological features in VMs were observed among the individuals having genetic mutations in VMs; thus, indicating gene-specific effects. Therefore, these features could suggest and support the presence of specific mutations in VMs. The analysis of detailed gene-specific effects in VMs offers insight into the underlying molecular pathways, and may provide an opportunity to identify selected targeted therapies in the future.

Ethics approval and consent to participate

This study was approved by the Ethical Review Board of the Graduate School of Medicine, Osaka University (IRB No. 17214) and was performed in accordance with the committee guidelines and regulations.

Consent for publication

The requirement for informed consent was waived by the Ethical Review Board.

Availability of data and materials

Data supporting the findings of this study are available upon request from the corresponding author.

Funding

This work was supported by JSPS KAKENHI (18K15079 and 21K15384), Children's Cancer Association of Japan, Futoku Foundation, Japan Intractable Diseases (Nanbyo) Research Foundation (2021B02), Kurozumi Medical Foundation, Mother and Child Health Foundation, Nishiyama Dental Academy General Foundation, Takeda Science Foundation, Osaka Medical Research Foundation for Intractable Diseases (28-2-34), and Uehara Memorial Foundation.

CRediT authorship contribution statement

Katsutoshi Hirose: Writing – review & editing, Writing – original draft, Visualization, Validation, Supervision, Resources, Project

administration, Methodology, Investigation, Funding acquisition, Data curation, Conceptualization. **Yumiko Hori:** Writing – review & editing, Writing – original draft, Visualization, Validation, Supervision, Resources, Project administration, Methodology, Investigation, Funding acquisition, Data curation, Conceptualization. **Michio Ozeki:** Supervision, Resources. **Daisuke Motooka:** Validation, Investigation. **Kenji Hata:** Investigation. **Shinichiro Tahara:** Supervision, Investigation. **Takahiro Matsui:** Supervision, Investigation. **Masaharu Kohara:** Resources, Investigation. **Kazuaki Maruyama:** Supervision. **Kyoko Imanaka-Yoshida:** Supervision. **Satoru Toyosawa:** Supervision, Resources. **Eiichi Morii:** Writing – review & editing, Writing – original draft, Visualization, Supervision, Resources, Project administration, Data curation, Conceptualization.

Declaration of competing interest

The authors declare that they have no known competing financial interests or personal relationships that could have appeared to influence the work reported in this paper.

Acknowledgements

We thank Ms Takako Sawamura, and Ms Megumi Nihei from the Department of Pathology, Osaka University Graduate School of Medicine for their technical assistance. Next-generation sequencing and Visium spatial transcriptomic analysis were performed by the Research Institute for Microbial Diseases (Osaka University). The authors would like to acknowledge the support of the staff. All authors contributed to this work and reviewed and approved the manuscript for submission.

Appendix A. Supplementary data

Supplementary data to this article can be found online at https://doi.org/10.1016/j.humpath.2024.02.004.

References

[1] ISSVA classification for vascular anomalies: Available from: https://www.issva.org/UserFiles/file/ISSVA-Classification-2018.pdf. Accessed 10 December 2023.
[2] Dompmartin A, Vikkula M, Boon LM. Venous malformation: update on aetiopathogenesis, diagnosis and management. Phlebology 2010;25:224–35.
[3] Colmenero I, Knöpfel N. Venous malformations in childhood: clinical, histopathological and genetics update. Dermatopathology 2021;8:477–93.
[4] Limaye N, Wouters V, Uebelhoer M, et al. Somatic mutations in angiopoietin receptor gene TEK cause solitary and multiple sporadic venous malformations. Nat Genet 2009;41:118–24.
[5] Ye C, Pan L, Huang Y, et al. Somatic mutations in exon 17 of the TEK gene in vascular tumors and vascular malformations. J Vasc Surg 2011;54:1760–8.
[6] Limaye N, Kangas J, Mendola A, et al. Somatic activating PIK3CA mutations cause venous malformation. Am J Hum Genet 2015;97:914–21.
[7] Castel P, Carmona FJ, Grego-Bessa J, et al. Somatic PIK3CA mutations as a driver of sporadic venous malformations. Sci Transl Med 2016;8:332–42.
[8] Castillo SD, Tzouanacou E, Zaw-Thin M, et al. Somatic activating mutations in Pik3ca cause sporadic venous malformations in mice and humans. Sci Transl Med 2016;8. 332–343.
[9] Du Z, Liu JL, You YH, et al. Genetic landscape of common venous malformations in the head and neck. J. Vas. Surg. Venous Lymphatic Disorders 2021;9. 1007–16.e7.
[10] Morris PN, Dunmore BJ, Tadros A, et al. Functional analysis of a mutant form of the receptor tyrosine kinase Tie2 causing venous malformations. J Mol Med 2005;83:58–63.
[11] Du Z, Zheng J, Zhang Z, Wang Y. Review of the endothelial pathogenic mechanism of TIE2-related venous malformation. Journal of Vascular Surgery. Venous and Lymphatic Disorders 2017;5:740–8.
[12] Kangas J, Nätynki M, Eklund L. Development of molecular therapies for venous malformations. Basic Clin Pharmacol Toxicol 2018;123(Suppl 5):6–19.
[13] Nätynki M, Kangas J, Miinalainen I, et al. Common and specific effects of TIE2 mutations causing venous malformations. Hum Mol Genet 2015;24:6374–89.
[14] Boscolo E, Limaye N, Huang L, et al. Rapamycin improves TIE2-mutated venous malformation in murine model and human subjects. J Clin Invest 2015;125:3491–504.
[15] Goines J, Li X, Cai Y, et al. A xenograft model for venous malformation. Angiogenesis 2018;21:725–35.
[16] Uebelhoer M, Nätynki M, Kangas J, et al. Venous malformation-causative TIE2 mutations mediate an AKT-dependent decrease in PDGFB. Hum Mol Genet 2013;22:3438–48.
[17] Li X, Cai Y, Goines J, et al. Ponatinib combined with rapamycin causes regression of murine venous malformation. Arterioscler Thromb Vasc Biol 2019;39:496–512.
[18] Chen GH, Yang JG, Xia HF, et al. Endothelial cells induce degradation of ECM through enhanced secretion of MMP14 carried on extracellular vesicles in venous malformation. Cell Tissue Res 2022;389:517–30.
[19] Van Damme A, Seront E, Dekeuleneer V, Boon LM, Vikkula M. New and emerging targeted therapies for vascular malformations. Am J Clin Dermatol 2020;21:657–68.
[20] Queisser A, Seront E, Boon LM, Vikkula M. Genetic basis and therapies for vascular anomalies. Circ Res 2021;129:155–73.
[21] Hammer J, Seront E, Duez S, et al. Sirolimus is efficacious in treatment for extensive and/or complex slow-flow vascular malformations: a monocentric prospective phase II study. Orphanet J Rare Dis 2018;13:191.
[22] Freixo C, Ferreira V, Martins J, et al. Efficacy and safety of sirolimus in the treatment of vascular anomalies: a systematic review. J Vasc Surg 2020;71:318–27.
[23] Maruani A, Tavernier E, Boccara O, et al. Sirolimus (rapamycin) for slow-flow malformations in children: the observational-phase randomized clinical PERFORMUS trial. JAMA Dermatol 2021;157:1289–98.
[24] Hori Y, Ozeki M, Hirose K, et al. Analysis of mTOR pathway expression in lymphatic malformation and related diseases. Pathol Int 2020;70:323–9.
[25] Hori Y, Hirose K, Aramaki-Hattori N, et al. Fibro-adipose vascular anomaly (FAVA): three case reports with an emphasis on the mammalian target of rapamycin (mTOR) pathway. Diagn Pathol 2020;15:98.
[26] Hori Y, Hirose K, Ozeki M, et al. PIK3CA mutation correlates with mTOR pathway expression but not clinical and pathological features in fibroadipose vascular anomaly (FAVA). Diagn Pathol 2022;17:19.
[27] Canaud G, Hammill AM, Adams D, Vikkula M, Keppler-Noreuil KM. A review of mechanisms of disease across PIK3CA-related disorders with vascular manifestations. Orphanet J Rare Dis 2021;16:306.
[28] Pore N, Liu S, Shu HK, et al. Sp1 is involved in Akt-mediated induction of VEGF expression through an HIF-1-independent mechanism. Mol Biol Cell 2004;15:4841–53.
[29] Si Y, Huang J, Li X, et al. AKT/FOXO1 axis links cross-talking of endothelial cell and pericyte in TIE2-mutated venous malformations. Cell Commun Signal 2020;18:139.